J|A|C|S
ARTICLES
Published on Web 06/02/2004

Variation of Ser-L223 Hydrogen Bonding with the Q_B Redox State in Reaction Centers from *Rhodobacter sphaeroides*

Hiroshi Ishikita and Ernst-Walter Knapp*

Contribution from the Institute of Chemistry, Department of Biology, Chemistry, and Pharmacy, Free University of Berlin, Takustrasse 6, D-14195 Berlin, Germany

Received August 24, 2003; E-mail: knapp@chemie.fu-berlin.de

Abstract: Ser-L223 is close to ubiquinone (Q_B) in the B-branch of the bacterial photosynthetic reaction center (bRC) from *Rhodobacter* (*Rb*) *sphaeroides*. Therefore, the presence of a hydrogen bond (H bond) between the two was naturally proposed from the crystal structure. The hydrogen bonding pattern of Q_B from the light-exposed structure was studied by generating hydrogen atom coordinates based on the CHARMM force field. In the Q_B neutral charge state (Q_B^0), no H bond was found between the oxygen of the OH group from Ser-L223 and the carbonyl oxygen of Q_B that is distal to the non-heme iron. In the reduced state (Q_B^-), however, Ser-L213 was found to form an H bond with Q_B only when Asp-L213 is protonated by more than 0.75 H^+. This indicates the significance of the protonation of Asp-L213 in forming an H bond between Ser-L223 and Q_B. We found that the driving force to form the H bond between Ser-L223 and Q_B is enhanced by the positively charged Arg-L217. The calculated Q_B redox potentials with or without this H bond discriminated two ET rates, which are close to the faster and slower time phases observed in UV−Vis and FTIR studies. Together with the calculated redox potential of the quinones, this H-bond formation could play a key role in conformational gating for the ET process from Q_A to Q_B.

Introduction

The primary event in bacterial photosynthetic reaction centers (bRC) after electronic excitation of the bacteriochlorophyll (BChl) dimer, the special pair (SP), is a charge-separation process. As a result, the SP becomes oxidized while an electron is transferred along the A-branch cofactors from an accessory BChl via bacteriopheophytin, to ubiquinone (ubi-Q) Q_A in the A-branch and subsequently to Q_B in the B-branch. The electron transfer (ET) process from Q_A to Q_B, which is coupled with a proton uptake reaction at Q_B, is repeated, yielding finally the protonated dihydroquinone Q_BH_2 that leaves the binding pocket and is replaced by another quinone from the pool. Recently, it was suggested that before the first ET from Q_A to Q_B the bRC undergoes a conformational change from an ET-inactive to an ET-active form.[1] In the dark-adapted structure (ET-inactive), Q_B is displaced by 5 Å relative to its position in the light-exposed structure (ET-active) and has undergone a propeller twist by 180°.[1] In the dark-adapted structure, only a single H bond of the Q_B^0 carbonyl oxygen distal to the non-heme iron ($O_{distal}(Q_B)$) with the amide backbone of Ile-L224 (N−O distance 3.1 Å) is present.[1,2] In the light-exposed structure, the distal carbonyl oxygen of Q_B^- is involved in three branched H bonds with the amide backbone of Ile-L224 (N−O distance 3.0 Å), Gly-L225 (N−O distance 3.3 Å), and the Ser-L223 OH group (O−O distance 3.2 Å) as suggested from the crystal structure, while the proximal carbonyl oxygen of Q_B forms a single strong H bond with the N_δ nitrogen of His-L190 (N−O distance 2.8 Å) [1].

After the first ET process, Q_B^- becomes protonated, forming Q_BH that is stabilized by the second ET.[3] Although His-H126, His-H128, Asp-M17, Asp-L210, Asp-L213, and Ser-L223 were suggested to be involved in proton-transfer events,[3,4] it is an open question how the proton arrives at the Q_B binding site. In the present study, we report a local change of H-bond pattern involving Q_B and Ser-L223 that is governed by the redox state of Q_B.

Computational Procedures

Coordinates. In our computations, we used the light-exposed structure of the bRC from *Rhodobacter* (*Rb*) *sphaeroides*.[1] The atomic coordinates were prepared in the same way as in previous applications.[5,6] The position of hydrogen atoms were energetically optimized with the CHARMM force field,[7] while the positions of all non-hydrogen atoms were fixed, all titratable groups except for Glu-L212 and Asp-L213 were kept in their standard charge state; i.e., basic groups were considered to be protonated, and acidic groups, ionized. Coordinates of the non-hydrogen atoms were used as given in the crystal structure. In the optimization procedure of hydrogen atom coordinates, the dielectric constant was set to unity as is usually done in conventional CHARMM applications for geometry optimization or molecular dynamics simulation of biomolecular systems. However, focusing on

(1) Stowell, M. H. B.; McPhillips, T. M.; Rees, D. C.; Solitis, S. M.; Abresch, E.; Feher, E. *Science* **1997**, *276*, 812−816.
(2) Ermler, U.; Fritzsch, G.; Buchanan, S. K.; Michel, H. *Structure* **1994**, *2*, 925−936.
(3) Graige, M. S.; Paddock, M. L.; Bruce, J. M.; Feher, G.; Okamura, M. Y. *J. Am. Chem. Soc.* **1996**, *118*, 9005−9016.
(4) Gerencser, L.; Maroti, P. *Biochemistry* **2001**, *40*, 1850−1860.
(5) Rabenstein, B.; Ullmann, G. M.; Knapp, E. W. *Biochemistry* **2000**, *39*, 10487−10496.
(6) Ishikita, H.; Morra, G.; Knapp, E. W. *Biochemistry* **2003**, *42*, 3882−3892.
(7) Brooks, B. R.; Bruccoleri, R. E.; Olafson, B. D.; States, D. J.; Swaminathan, S.; Karplus, M. J. *Comput. Chem.* **1983**, *4*, 187−217.

the energetics of variably charged titratable or redox-active molecular groups in proteins where only a single protein conformation of non-hydrogen atoms is considered, the usage of a dielectric constant of $\epsilon_P = 4$ turned out to be most suitable. Atomic partial charges of the amino acids were adopted from the all-atom CHARMM22 [8] parameter set. For cofactors and residues whose charges are not available in CHARMM22, we used atomic partial charges from previous applications.[5,6] Generally, there is no explicit experimental information available on hydrogen atom positions of water molecules found in protein crystal structures. Generating these coordinates by modeling methods depends critically on the protonation pattern of titratable residues, and often more than one conformation is possible. To avoid these ambiguities, we did not treat water molecules explicitly and removed all crystal waters as was done in most of our previous applications.[5,6] Hence, most of the results in the present application were computed in absence of explicit water molecules if not otherwise stated. But, to check the influence of explicit water molecules, a geometry optimization of hydrogen atoms was also performed in the presence of all crystal waters using the TIP3P water model.[9]

Computation of Quinone Redox Potential. The computation of the energetics of the protonation pattern is based on the electrostatic continuum model by solving the linear Poisson Boltzmann (LPB) equation with the program MEAD from Bashford and Karplus.[10] The ensemble of protonation patterns was sampled by a Monte Carlo (MC) method where we used our own program Karlsberg.[11] In the first 3000 MC scans, the protonation states of all titratable residues were changed individually by random selection on the average 3000 times. In the subsequent 7000 MC scans, the protonation state was fixed for all titratable residues whose protonation state deviated by less than 10^{-6} protons from fully protonated or deprotonated. The detailed procedure that we used is described in refs 5, 6, and 12. The dielectric constant was set to $\epsilon_P = 4$ inside the protein and $\epsilon_W = 80$ for water. Crystal waters that were removed from a protein structure left cavities where the dielectric constant was set to $\epsilon_W = 80$. Accordingly, the effect of the removed water molecules was considered implicitly by the high value of the dielectric constant in these cavities. A discussion on the appropriate value of the dielectric constant in proteins can be found in refs 13−17. All computations were performed at 300 K with pH 7.0 and an ionic strength of 100 mM. The LPB equation was solved using a three-step grid-focusing procedure with a starting grid resolution of 2.5 Å, an intermediate grid resolution of 1.0 Å, and a final grid resolution of 0.3 Å. MC sampling yields the probabilities $[A_{ox}]$ and $[A_{red}]$ of oxidized and reduced state of the redox-active group A, respectively. With these probabilities, the redox potentials can be calculated from the Nernst equation,

$$E = E^\circ + \frac{RT}{F}\ln\frac{[A_{ox}]}{[A_{red}]} \quad (1)$$

where F is the Faraday constant, E is the solution redox potential, and E° is the standard redox potential of the redox-active group A. For convenience, the computed redox potentials are given with mV accuracy; albeit this does not suggest that the last digit is significant. For further information about the procedure of redox potential computation and error estimate, see ref 18. The value of −360 mV for the redox potential of ubi-Q in DMF 6 versus normal hydrogen electrode was taken from the same reference[19] as was the redox potential of phylloquinone (phyllo-Q) used in our previous application for PSI.[18] This may help to clarify uncertainties arising from different conditions to measure these redox potentials. It also facilitates a direct comparison of our calculated phyllo-Q (A_1) redox potentials in PSI [18] with the calculated ubi-Q redox potentials obtained in bRC.

Fractional versus Pure Protonation and Conformational Transitions. Titratable residues can only be in a fully protonated or deprotonated charge state (pure protonation). With the MC sampling procedure, exactly these charge states of titratable residues in proteins are collected. However, different protonation patterns may go along also with different conformations. The present computational procedure is conservative with respect to conformational changes as was done in previous applications.[5,6] More general treatments that considered specifically selected conformations simultaneously with charge pattern variation were with some exceptions of limited success. One reason may be the problem to find a representative ensemble of conformations. Consequently, we keep the atomic coordinates from the crystal structure for different protonation patterns. Coordinates of the variable protons from titratable residues are also treated conservatively as in previous applications.[5,6] In the deprotonated state of the basic residues, Arg and Lys, the variable proton was not removed but the charges of the equivalent polar protons were symmetrically reduced by a net unit charge. Similarly, no explicit proton was used for the protonated state of the acidic residues, Asp and Glu, but the charges of the two carboxylic oxygens were symmetrically enhanced by a net unit charge. Thus, ambiguities in removal or placement of a variable proton are avoided, and simultaneously averaging over different variable proton conformations is approximately performed by using these symmetrized conformations.

To study the influence of protonation pattern on the H-bond scheme of specific molecular groups such as the OH group of serine or tyrosine, conventional methods of structural relaxation like energy minimization require a specific charge pattern. Therefore, in the case of partial protonation or deprotonation, we use fractional charges, which were obtained by interpolation between the two limiting charge states (protonated and deprotonated). This approximate treatment is fully justified, if the protonation−deprotonation equilibrium of the corresponding titratable residue adjusts fast compared to the considered change in conformation, which is in the present case a change in H-bond pattern. Even in the case where the conformations adjust fast to the change in protonation state, results remain qualitatively meaningful. This is for instance the case if one observes a conformational change going along with the transition from a pure to a fractional protonation state.

ET Rate between Quinones Based on Computed Redox Potentials. ET rates in proteins can be estimated by the following empirical expressions, which describe ET processes between cofactors for exergonic (energetically downhill) and endergonic (energetically uphill) ET processes, respectively.[20]

$$k_{T=300K}^{\text{exergonic ET}} = \exp\{13 - 0.6(R - 3.6) - 3.1(-|\Delta G| + \lambda)^2/\lambda\} \quad (2)$$

$$k_{T=300K}^{\text{endergonic ET}} = \exp\{13 - 0.6(R - 3.6) - 3.1(-|\Delta G| + \lambda)^2/\lambda - |\Delta G|/0.06\} \quad (3)$$

(8) MacKerell, A. D. J.; Bashford, D.; Bellott, M.; Dunbrack, R. L., Jr.; Evanseck, J. D.; Field, M. J.; Fischer, S.; Gao, J.; Guo, H.; Ha, S.; D. Joseph-McCarthy, D.; Kuchnir, L.; Kuczera, K.; Lau, F. T. K.; Mattos, C.; Michnick, S.; Ngo, T.; Nguyen, D. T.; Prodhom, B.; Reiher, W. E., III; Roux, B.; Schlenkrich, M.; Smith, J. C.; Stote, R.; Straub, J.; Watanabe, M.; Wiórkiewicz-Kuczera, J.; Yin, D.; Karplus, M. *J. Phys. Chem. B* **1998**, *102*, 3586−3616.
(9) Jorgensen, W. L.; Chandrasekhar, J.; Madura, J. D. *J. Chem. Phys.* **1983**, *79*, 926−935.
(10) Bashford, D.; Karplus, M. *Biochemistry* **1990**, *29*, 10219−10225.
(11) Rabenstein, B. Karlsberg online manual 1999, http://agknapp.chemie.fu-berlin.de/karlsberg/.
(12) Rabenstein, B.; Ullmann, G. M.; Knapp, E. W. *Biochemistry* **1998**, *37*, 2488−2495.
(13) Rabenstein, B.; Ullmann, G. M.; Knapp, E. W. *Eur. Biphys. J.* **1998**, *27*, 626−637.
(14) Honig, B.; Nicholls, A. *Science* **1995**, *268*, 1144−1149.
(15) Warshel, A.; Russel, S. T. Q. *Rev. Biophys.* **1984**, *17*, 283−422.
(16) Warshel, A.; Åqvist, J. *Annu. Rev. Biophys. Biophys. Chem.* **1991**, *20*, 267−298.
(17) Warshel, A.; Papazyan, A.; Muegge, I. *J. Biol. Inorg. Chem.* **1997**, *2*, 143−152.
(18) Ishikita, H.; Knapp, E. W. *J. Biol. Chem.* **2003**, 52002−52011.
(19) Prince, R. C.; Dutton, P. L.; Bruce, J. M. *FEBS Lett.* **1983**, *160*, 273−276.
(20) Page, C. C.; Moser, C. C.; Chen, X.; Dutton, P. L. *Nature* **1999**, *402*, 47−52.

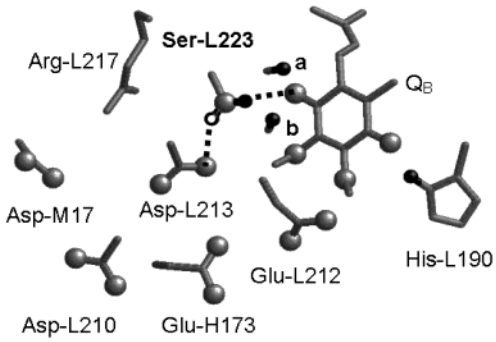

Figure 1. Residues in the neighborhood of the Q_B binding site with an H bond from Ser-L223 to Q_B (black sphere for hydrogen) or alternatively with the H bond from Ser-L223 to Asp-L213 (open circle). Hydrogen atoms are depicted by black spheres, and oxygen atoms, by gray spheres. For the other two residues Ile-L224 and Gly-L225 (a and b in the figure, respectively) that form H bonds with Q_B, only the backbone NH groups are displayed.

The reorganization energy is λ. The reaction free energy ΔG is the redox potential difference between the electron donor and acceptor group whose edge-to-edge distance is greater than $R = 3.6$ Å. Note that in these rate expressions energy parameters (ΔG and λ) are given in units of eV and distances (R) in units of Å. The edge-to-edge distance $R = 13.6$ Å between donor Q_A^- and acceptor Q_B^0 was taken from the light-exposed crystal structure.[1] Note that both edge-to-edge distances from Q_A and Q_B to the non-heme iron are equal to 6.8 Å, which coincides also with the distances from the two phyllo-Q to the iron−sulfur cluster F_X in PSI.[21] For the reorganization energy λ we took the value $\lambda = 0.85$ eV estimated from a UV−Vis study of the ET process from Q_A to Q_B in bRC from *Rb. sphaeroides*.[22] This value is intermediate between 1.0 eV estimated for the ET from Q (A_1) to F_X in PSI [23] and the canonical value of 0.7 eV suggested for photosynthetic proteins.[24]

Results and Discussion

Charge States of Residues Responsible for the H Bond Formation between Ser-L223 and Q_B. With geometry optimization using the standard charge state of titratable residues (i.e., ionized for acidic and protonated for basic residues), two H bonds from the backbone nitrogens of Ile-L224 and Gly-L225 were observed with $O_{distal}(Q_B)$. These two H bonds formed in both quinone redox states (Q_B^0 and Q_B^-). But, in contrast to general expectations, the Ser-L223 OH group formed an H bond with the carbonyl oxygen of Asp-L213 instead with $O_{distal}(Q_B)$ for oxidized Q_B (i.e., Q_B^0) (Figure 1).

For the protonation states of Glu-L212 and Asp-L213, the general agreement is that Glu-L212 is fully or nearly fully protonated in both quinone redox states, $Q_A^0Q_B^0$ and $Q_A^0Q_B^-$. However, FTIR spectroscopy [25,26] and kinetic studies[27−29] indicated an ionized Asp-L213 in both redox states, while, from molecular dynamics simulations[30] and electrostatic computations,[5,6,31] it was concluded that Asp-L213 is protonated in the redox state $Q_A^0Q_B^-$. We investigated the possible protonation pattern of Glu-L212 and Asp-L213 by adding hydrogen atoms to the crystal structure of the bRC. We found that only when Asp-L213 is protonated in the Q_B^- state, the OH group of Ser-L223 forms a strong H bond with the quinone oxygen $O_{distal}(Q_B)$ distal to the non-heme iron (Figure 1). Interestingly, the formation of this H bond was independent of the Glu-L212 protonation state.

Recent electrostatic computations revealed that except for the three residues, Glu-L212, Asp-L213 and Asp-M17, no significant change in the protonation pattern was found for both redox states, $Q_A^0Q_B^0$ and $Q_A^0Q_B^-$.[6] Therefore, we investigated predominantly the charge state of Asp-L213 for the quinone charge state $Q_A^0Q_B^-$. For this purpose we used a fractional protonation of Asp-L213 as discussed in the method section. Increasing the fractional protonation of Asp-L213 to more than 0.75 H^+, we observed the breaking of the H bond between Ser-L223 and Asp-L213 and simultaneously the formation of the H bond between Ser-L223 and $O_{distal}(Q_B)$. Although the fractional protonation of Asp-L213 is an approximation as discussed in the method section, the observed change in the H-bonding scheme remains conclusive. Interestingly, a value larger than 0.75 H^+ for the protonation of Asp-L213 was suggested recently based on electrostatic energy computations to guarantee that the ET from Q_A to Q_B is downhill in energy.[6] Note that the other two H bonds of Q_B^- with the backbone nitrogen of Ile-L224 and Gly-L225 were not affected by a change in the protonation state of Asp-L213. Together with FTIR studies that indicated no proton uptake at Asp-L213,[25,26] we suggested that Asp-L213 should remain protonated during the entire ET process.[6] Since the crystal structure obtained under illumination[1] corresponds to the $Q_A^0Q_B^-$ state, our result supports the existence of three simultaneous branched H bonds to $O_{distal}(Q_B)$ in the $Q_A^0Q_B^-$ state involving Ile-L224, Gly-L225, and also Ser-L223. Hence, the initiation process for the exergonic (energetically downhill) ET process from Q_A to Q_B is the formation of the H bond between Ser-L223 and Q_B^-.

Asp-L213 Charge State as Driving Force To Form the H Bond from Ser-L223 to Q_B. We found a dependence of the H-bond pattern on the charge state of Asp-L213 where the following two limiting cases can be discriminated: (i) If Asp-L213 is protonated by 0.75 H^+, the H bond between Ser-L223 and Q_B occurs only for fully reduced Q_B. However, this H bond breaks already if Q_B is 90% reduced. In this case, we observe the H bond between Ser-L223 and Asp-L213, which is also present for fully oxidized Q_B (i.e., Q_B^0). (ii) For fully protonated Asp-L213, the H bond from Ser-L223 to Q_B forms already when the ET reaction is only 55% complete. At 50% completion, the O−H distances of Ser-L223 to $O_{distal}(Q_B)$ and to O(Asp-L213) are nearly identical. Hence, for fully protonated Asp-L213, the driving force to form the H bond from Ser-L223 to Q_B seems to be much stronger than that for Asp-L213 protonated by 0.75 H^+, which implies that the formation of the H bond from Ser-L223 to Q_B and the ET process should be synchronized. In that respect, a fully protonated Asp-L213 may energetically be more favorable for the ET process from Q_A to Q_B than Asp-L213

(21) Jordan, P.; Fromme, P.; Witt, H. T.; Klukas, O.; Saenger, W.; Krauss, N. *Nature* **2001**, 411, 909−917.
(22) Li, J.; Takahashi, E.; Gunner, M. R. *Biochemistry* **2000**, *39*, 7445−7454.
(23) Schlodder, E.; Falkenberg, K.; Gergeleit, M.; Brettel, K. *Biochemistry* **1998**, *37*, 9466−9476.
(24) Moser, C. C.; Keske, J. M.; Warncke, F.; Farid, R. S.; Dutton, P. L. *Nature* **1992**, *355*, 796−802.
(25) Nabedryk, E.; Breton, J.; Hienerwadel, R.; Fogel, C.; Mäntele, W.; Paddock, M. L.; Okamura, M. Y. *Biochemistry* **1995**, *34*, 14722−12732.
(26) Nabedryk, E.; Breton, J.; Okamura, M. Y.; Paddock, M. L. *Biochemistry* **1998**, *37*, 14457−14462.
(27) Takahashi, E.; Wraight, C. A. *Biochim. Biophys. Acta* **1990**, *1020*, 107−111.
(28) Takahashi, E.; Wraight, C. A. *Biochemistry* **1992**, *31*, 855−866.
(29) Paddock, M. L.; Rongey, S. H.; McPherson, P. H.; Juth, A.; Feher, G.; Okamura, M. Y. *Biochemistry* **1994**, *33*, 734−745.
(30) Grafton, A. K.; Wheeler, R. A. *J. Phys. Chem. B* **1999**, *103*, 5380−5387.
(31) Alexov, E. G.; Gunner, M. R. *Biochemistry* **1999**, *38*, 8253−8270.

protonated by 0.75 H^+. In fact, further electrostatic computations in the present study support Asp-L213 to be fully protonated in the quinone redox states $Q_A^-Q_B^0$ and $Q_A^0Q_B^-$, implying that the Asp-L213 0.75 H^+ protonation is just a minimum requirement to provide enough driving force for the H-bond formation from Ser-L223 to Q_B.

The computations were also performed with explicit crystal water yielding a marginally different result in forming the H bond between Ser-L223 and Q_B^-. Here, with Asp-L213 in the protonation state 0.75 H^+, Ser-L223 was already H bonded to the 90% reduced Q_B, while, in the absence of crystal water, Q_B was needed in the fully reduced state to form this H bond. This indicates that the model with explicit water exhibits a slightly enhanced driving force for H-bond formation between Ser-L223 and Q_B. But, such small differences are in the uncertainty margin of force field computations and also of possible experiments.

Influence of Arg-L217 on the Ser-L223 H Bond. Arg-L217, which is also in the neighborhood of Ser-L223, may have an influence on the H bond of Ser-L223 due to its net positive charge (Figure 1). Setting the charge on this residue to zero weakens the H bond of Ser-L223 to Q_B considerably (O − H distance of 3.3 Å) even in the presence of a fully reduced Q_B^- and fully protonated Asp-L213, albeit the O−H distance is still shorter than the one in the presence of Q_B^0 and fully ionized Asp-L213 (O−H distance 4.0 Å). Hence, these results support an experimental study on double mutated bRC [Ser-L223→Ala/Arg-L217→His] where a significant decrease of Q_B binding constant was found, diminishing from 4.5 μM in the wild-type to 0.5 μM in the mutant bRC.[32] Kinetic studies indicated that the mutation of Arg-L217 to isoleucine decreased the effective concentration of protons (proton activity) at the Q_B site.[33] Together with our results, we can conclude that, in the absence of the positive charge at Arg-L217, Ser-L223 and Q_B^- are not able to form a strong H bond. Hence, the presence of Arg-L217 may increase the driving force to form the H bond between Ser-L223 and Q_B and thus also increase the driving force of the ET process from Q_A to Q_B.

Dependence of Q_B Redox Potential on H Bond with Ser-L213. The H bond between Ser-L223 and Q_B is expected to upshift the Q_B redox potential due to the stabilization effect of the Q_B^- charge state. To quantitatively check this influence, we calculated the redox potentials of Q_B in the presence or absence of the H bond from Ser-L223 to Q_B. Note that in the latter case Ser-L223 forms an H bond to Asp-L213 instead to Q_B as discussed in the preceding sections.

In our computations, the redox potentials were calculated to be −171 mV and −125 mV for Q_A and Q_B, respectively, in the presence of the H bond with Ser-L223. Note that the calculated Q_A redox potential corroborates the value of −180 mV obtained from redox titration in chromatophores[34−36] and also in isolated bRC.[37] The reaction free energy of the ET process from Q_A to Q_B is energetically downhill with −46 meV. This is in good agreement with the value of −52 meV observed in kinetic studies.[38]

Table 1. Protonation Pattern of Glu-L212 and Asp-L213 in the Wild-Type bRC Dependent on the Quinone Charge Pattern

quinone charges	$Q_A^-Q_B^0$		$Q_A^0Q_B^-$		$Q_A^0Q_B^0$	
Ser-L223 H bond	+H[a]	–H[b]	+H	–H	+H	–H
Glu-L212	0.02	0.12	1.00	1.00	0.00	0.02
Asp-L213	1.00	0.89	1.00	0.99	1.00	0.97

[a] bRC with the H bond between Ser-L223 and Q_B. [b] bRC without the H bond between Ser-L223 and Q_B.

On the other hand, in the absence of an H bond of Q_B with Ser-L223, the Q_B redox potential was downshifted to the new value of −231 mV, while the Q_A redox potential remained practically unchanged at −168 mV. Thus, a removal of the H bond between Ser-L223 and Q_B would dramatically change the driving force of the ET process from an energetically downhill (−46 meV) to an uphill (+63 meV) reaction.

The protonation pattern in bRC was calculated for the three quinone redox states $Q_A^-Q_B^0$, $Q_A^0Q_B^-$, and $Q_A^0Q_B^0$, yielding practically identical protonation patterns for both H-bond realizations of Ser-L223. Glu-L212 becomes protonated upon changing the redox state from $Q_A^-Q_B^0$ to $Q_A^0Q_B^-$, while Asp-L213 remains protonated (Table 1). The identical protonation pattern in both of the H-bond conformers is in particular also valid for Asp-L210, Asp-M17, Asp-H124, and Glu-H173, which are supposed to participate in the proton-transfer pathway from the surface entry point to Q_B (Figure 1). These residues were found to remain ionized in all three quinone redox states. (Note that by a misprint in ref 6 it was erroneously stated that Glu-H173 was found to be protonated.) Therefore, the significant difference of the Q_B redox potential obtained from calculations based on the bRC structures with and without the H bond from Ser-L223 to Q_B is not due to a global change in the protonation pattern at the Q_B site but merely due to the structural difference in the orientation of the Ser-L223 OH group pointing either to Q_B or to Asp-L213.

Influence of the H Bond from Ser-L223 on the ET Rate. The attribution of the different time phases observed for the ET process from Q_A to Q_B in bRC is still a matter of debate. UV−Vis studies show a biphasic ET process with characteristic time constants of 25−67 μs and 200−250 μs,[22,39−42] where the faster phase represents about 60% of the Q_B^- yield, while the remaining 40% correspond to the slower phase. On the other hand, three time phases of 12 μs, 150 μs, and 1.1−1.2 ms were observed in FTIR studies.[43,44] Note that the two faster phases observed in FTIR studies correspond to the faster phase and slower phase in the UV−Vis studies. In a recent FTIR study on the ET process from Q_A to Q_B, no notable oxidation of Q_A was found to take place in the time range of 12 μs (equivalent to the phase of 25−67 μs in UV−Vis).[44] Hence, contrary to a general idea of Q_A as the electron donor of Q_B, it was suggested that another electron donor provides the electron to reduce Q_B. They proposed that possible candidate could be the non-heme

(32) Baciou, L.; Sinning, I.; Sebban, P. *Biochemistry* **1991**, 30, 9110−9116.
(33) Cherepanov, D. A.; Bibikov, S. I.; Bibikova, M. V.; Bloch, D. A.; Drachev, L. A.; Gopta, O. A.; Oesterhelt, D.; Semenov, A. Y.; Mulkidjanian, A. Y. *Biochim. Biophys. Acta* **2000**, *1459*, 10−34.
(34) Arata, H.; Parson, W. W. *Biochim. Biophys. Acta* **1981**, *638*, 201−209.
(35) Arata, H.; Nishimura, M. *Biochim. Biophys. Acta* **1983**, *726*, 394−401.
(36) Prince, R. C.; Dutton, P. L. *Arch. Biochem. Biophys*. **1976**, *172*, 329−334.
(37) Maróti, P.; Wraight, C. W. *Biochim. Biophys. Acta* **1988**, *934*, 329−347.
(38) Tandori, J.; Sebban, P.; Michel, H.; Baciou, L. *Biochemistry* **1999**, *38*, 13179−13187.
(39) Tiede, D. M.; Vazquez, J.; Cordova, J.; Marone, P. A. *Biochemistry* **1996**, *35*, 10763−10775.
(40) Graige, M. S.; Feher, G.; Okamura, M. Y. *Proc. Natl. Acad. Sci. U.S.A.* **1998**, *95*, 11679−11684.
(41) Li, J.; Gilroy, D.; Tiede, D. M.; Gunner, M. R. *Biochemistry* **1998**, *37*, 2818−2829.
(42) Tiede, D. M.; Utschig, L.; Hanson, D. K.; Gallo, D. M. *Photosynth. Res.* **1998**, *55*, 267−273.
(43) Brudler, R.; Gerwert, K. *Photosynth. Res*. **1998**, *55*, 261−266.
(44) Remy, A.; Gerwert, K. *Nat. Struct. Biol*. **2003**, *10*, 637−644.

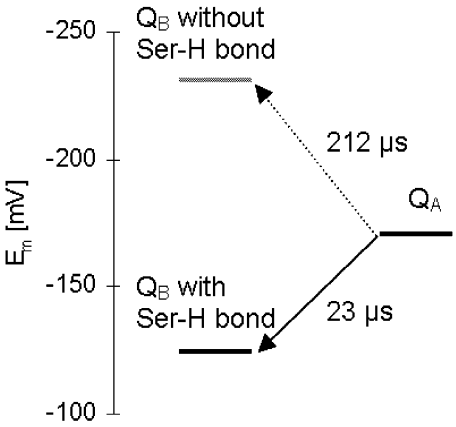

Figure 2. Reaction energy of the ET process from Q_A to Q_B given in terms of quinone redox potentials in the presence or the absence of the H bond between Ser-L223 and Q_B.

iron or one of its ligands, Glu-M234. However, in a UV−Vis study, the depletion of the non-heme iron resulted in a decrease of the ET rate constant by only a factor of 2.[45]

Based on our calculated redox potentials of both quinones, the ET rate was estimated for the bRC with and without H bond from Ser-L223 to Q_B according to eqs 2 and 3, respectively. We obtained a time constant of 23 μs for the ET from Q_A to Q_B in the presence of the H bond from Ser-L223 to Q_B, while a larger value of 212 μs was obtained in the absence of the H bond (Figure 2). The former time constant would correspond to the fastest phase observed in UV−Vis and FTIR studies while the latter is close to the slower phase. Hence, our estimated ET rates would suggest that the bRC is potentially ET active with and without the H bond between Ser-L223 and Q_B, indicating that the formation of the H bond between Ser-L223 and Q_B may not be necessary for the ET from Q_A to Q_B to occur. Accordingly, there are two different conformers of bRC with respect to the H-bond pattern of Q_B. In fact, FTIR measurements suggested that the carbonyls of Q_B in bRC interact with the protein environment 75% strongly and 25% weakly.[46] Together with the present results, one may conclude that the majority of bRC possesses an H bond between Ser-L223 and Q_B, while in the others the serine forms an H bond with Asp-L213. Interestingly, this ratio of the two conformers is close to the ratio found in UV−Vis studies, where 60% (40%) of the ET reaction belongs to the faster (slower) time phase.[22,41,42]

To confirm this hypothesis, we modeled the S(L223)A mutant bRC structure based on the wild-type light-exposed structure.[1] According to EPR spectra, the distance between Q_B and the non-heme iron in this mutant was not significantly altered from the wild-type bRC,[47] which could corroborate our modeling. Due to the replacement of the serine side chain by the nonpolar alanine, the mutant bRC should consist in a single conformer with respect to the H-bonding pattern for Q_B. The calculated redox potential of Q_B for the S(L223)A mutant was −183 mV, which is between the two values obtained for the two Ser-L223 H-bond conformers of the wild-type bRC. The Q_A redox potential did not change from the value in the wild-type bRC (−168 mV). With eq 3, the ET rate of this mutant was estimated to be 63 μs, in perfect agreement with the value of 67 μs obtained in the UV−Vis studies for this mutant.[47,48] Therefore, it seems likely that the H bond between Ser-L223 and Q_B is not indispensable for the ET process from Q_A to Q_B to occur but may play a crucial role in the reaction kinetics. In summary, the H-bond pattern from Ser-L223 to Q_B or to Asp-L213 significantly alternates the kinetic phases of the ET reaction between the quinones in the bRC.

Table 2. Protonation Pattern of Glu-L212 and Asp-L213 in the S(L223)A Mutant bRC Dependent on the Quinone Charge Pattern

quinone charges	$Q_A^-Q_B^0$	$Q_A^0Q_B^-$	$Q_A^0Q_B^0$
Glu-L212	0.02	0.00	0.00
Asp-L213	0.99	1.00	1.00

Protonation Pattern in the S(L223)A Mutant. In our computations the S(L223)A mutant exhibited a significantly different protonation pattern with respect to the wild-type bRC, predominantly in the neighborhood of Glu-L212. Instead of the transition from a fully ionized to a fully protonated Glu-L212 that we observed with a change in the redox state from Q_B^0 to Q_B^- in wild-type bRC (Table 1), this residue remains fully ionized in all Q_AQ_B redox states of the S(L223)A mutant (Table 2). Thus, for this mutant bRC Glu-L212 is unlikely to be involved in the proton uptake events of Q_B. The O−O distance of the side chain oxygens of Glu-L212 and Ser-L223 is larger than 8 Å. Nevertheless, our results suggest a strong interaction between the acidic residue Glu-L212 and the polar residue Ser-L223 in the wild-type bRC, while no such interaction is possible with the nonpolar residue Ala-L223 in the mutant. A kinetic study suggested that the rate of the proton-coupled ET process ($Q_A^-Q_B^- + H^+ \rightarrow Q_AQ_BH^-$) decreases dramatically by about a factor of 300 upon the S(L223)A mutation,[48] which according to our calculated protonation pattern can be interpreted by changing the role of Glu-L212 in proton uptake events at Q_B.

Conformational Gating of the ET Process. According to the concept of conformational gating, the distal Q_B position in the dark-adapted structure of the wild-type bRC was considered to be the ET-inactive form,[40] as was corroborated by electrostatic energy computations.[5,6,31] From a recent electrostatic energy computation on bRC by Taly et al.,[49] it was concluded that the conformation of Q_B depends on pH such that above pH 9 Q_B occupies only the proximal (light-exposed) site and below pH 6.5 occupies only the distal (dark-adapted) site. Consequently, the bRC should be ET-inactive below pH 6.5. However, ET was observed also at pH 6.0.[22] Contrary to the crystal structure, FTIR studies suggested a unique binding site of Q_B at the proximal position in the wild-type bRC in both Q_B^0 and Q_B^- charge states.[50] If the conformational gating would be controlled by the movement of Q_B, the rate of the ET from Q_A to Q_B should be dependent on the length of the Q_B isoprene chain. However, the ET rate remained unchanged in those experiments.[22,51,52]

(45) Debus, R. J.; Feher, G.; Okamura, M. Y. *Biochemistry* **1986**, *25*, 2276−2287.
(46) Brudler, R.; de Groot, H. J. M.; van Liemt, W. B. S.; Hoff, A. J.; Lugtenburg, J. L.; Gerwert, K. *FEBS Lett.* **1995**, *370*, 88−92.
(47) Paddock, M. L.; McPherson, P. H.; Feher, G.; Okamura, M. Y. *Proc. Natl. Acad. Sci. U.S.A.* **1990**, *87*, 6803−6807.
(48) Paddock, M. L.; Feher, G.; Okamura, M. Y. *Biochemistry* **1995**, *34*, 15742−15750.
(49) Taly, A.; Sebban, P.; Smith, J. C.; Ullmann, G. M. *Biophys. J.* **2003**, *84*, 2090−2098.
(50) Breton, J.; Boullais, C.; Mioskowski, C.; Sebban, P.; Baciou, L.; Nabedryk, E. *Biochemistry* **2002**, *41*, 12921−12927.
(51) Xu, Q.; Baciou, L.; Sebban, P.; Gunner, M. R. *Biochemistry* **2002**, *41*, 10021−10025.
(52) McComb, J. C.; Stein, R. R.; Wraight, C. A. *Biochim. Biophys. Acta* **1990**, *1015*, 156−171.

Instead of the Q_B movement, Breton et al. proposed a change of the protein conformation or protonation state of titratable residues as a possible alternative gating mechanism.[50] Our present study revealed that the alternative formation of the H bond from Ser-L223 to Q_B or to Asp-L213 is closely coupled to the charge state of Q_B, suggesting also the possibility that the H-bond pattern contributes to the rate-limiting step in the ET reaction. Hence, the H-bond and protonation pattern rather than the Q_B movement may be the key to understanding the different kinetics of the ET process from Q_A to Q_B.

Conclusion

We investigated the H-bonding pattern of the OH group of Ser-L223, which up to now was considered to bind to the quinone Q_B carbonyl group distal to the non-heme iron regardless of the quinone charge state. We found a specific charge pattern for the formation and breaking of this H bond that is coupled with the reaction coordinate (i.e., the degree of reduction of Q_B) describing the ET process between the quinones. According to conventional force field computations under equilibrium conditions, this H bond is only present if Q_B is fully reduced and Asp-L213 is at least 75% protonated. But, in the presence of a fully protonated Asp-L213, it is sufficient that Q_B is only to 55% reduced to maintain this H bond. In all other cases, the Ser-L223 OH group forms an H bond with an acidic oxygen of Asp-L213. Interestingly, to obtain an energetically downhill ET process from Q_A to Q_B, an Asp-L213 protonation of at least 75% is required.[6] Note that the fractional charge states that we considered here can be understood as a mean field time average if the charge state is fluctuating fast or as a majority rule if the charge state is changed slow in comparison with the other conformational changes that are in the focus of consideration.

The presence of the positive charge of Arg-L217 stabilizes the H bond of Ser-L223 with Q_B considerably. This corroborates the reduced proton activity at Q_B observed in kinetic studies of the R(L217)I mutant bRC [33] and the diminished binding constant of Q_B for the double mutant S(L223)A/R(L217)H.[32]

The Q_B redox potential was downshifted dramatically from -125 mV to -231 mV by 106 mV if Ser-L223 forms an H bond with Asp-L213 instead with Q_B in the wild-type bRC. Considering the S(L223)A mutant bRC, the Q_B redox potential adopted an intermediate value of -183 mV, which is practically isoenergetic with the Q_A redox potential of -171 mV. Estimating the ET rates of wild-type bRC on the basis of these computed redox potentials, one obtains values that are close to the two time constants observed in UV$-$Vis and FTIR spectra. For the S(L223)A mutant bRC, the time constant of the single ET phase observed in UV$-$Vis spectroscopy agrees with the computed time constant. Hence, the two ET phases observed spectroscopically can be correlated with the different H-bond pattern of Ser-L223. The agreement of measured and computed ET rate for the S(L223)A mutant bRC suggests that an H bond between Ser-L223 and Q_B is not necessary for the ET process from Q_A to Q_B to occur. Although these two different H bonds of Ser-L223 were connected quantitatively with the two different time phases observed for the ET from Q_A to Q_B, this structural variation may also provide a clue for the understanding of the conformational gating of this ET process. Hence, the present result suggests an alternative idea to the gating mechanism that was previously connected with the Q_B movement from the dark-adapted to light-exposed crystal structure of the bRC.

Acknowledgment. We thank Drs. Donald Bashford and Martin Karplus for providing the programs MEAD and CHARMM, respectively. We thank the Deutsche Forschungsgemeinschaft (Sfb498, Forschergruppe 475, GRK80/2, GRK268, GRK788/1). H.I. is grateful for a fellowship from the DAAD.

JA038092Q